

Surface Ionization of Metastable Calcium Atoms

I. Bucay,^{1, a)} A. Helal,¹ and M. G. Raizen¹

Center for Nonlinear Dynamics and Department of Physics, The University of Texas at Austin, Austin, Texas 78712, USA

(Dated: 29 September 2020)

We report an experimental study of surface ionization of metastable calcium atoms on a hot polycrystalline tungsten surface in vacuum. We implemented a hollow-cathode discharge to excite a fraction of calcium atoms in an atomic beam to metastable states and collected the resulting calcium ions. We observed that metastable calcium atoms are ionized with a significantly greater efficiency than ground-state atoms, and the results suggest that virtually every metastable atom impacting the hot surface is ionized. These results demonstrate the potential of metastable atom surface ionization as a means of enriching calcium isotopes for applications in medicine, metrology, and fundamental science.

I. INTRODUCTION

When atoms with ionization energy I are adsorbed on a metal surface with electronic work function Φ , the degree of ionization of the atom, α , is given by the Saha-Langmuir equation:¹

$$\alpha = \frac{n_i}{n_0} = \frac{g_i}{g_0} e^{-(I-\Phi)/k_B T}, \quad (1)$$

where n_i is the flux of surface ions emitted from the surface, n_0 is the flux of desorbed neutrals, g_0 and g_i are the statistical weights of the atomic and first ionic ground states, respectively, and T is the temperature of the heated metal surface. Should the surface work function be comparable to or exceed I , a significant fraction of the incident neutral atoms will evaporate from the surface as ions. The efficiency of surface ionization is given by $\beta = \alpha/(1 + \alpha)$ and is defined as the ratio of ions emitted from the surface to the total flux of atoms incident on the surface.^{2,3}

The theoretical and experimental aspects of surface ionization have been thoroughly documented⁴⁻⁸ and this phenomenon has been implemented as a detection tool for atomic beams,² as an ion source,^{9,10} and as a means of determining the ionization energy of exotic elements.^{11,12} Since the work function of refractory metals is no greater than ~ 6 eV, surface ionization has largely been limited to the alkali elements. In this article, we report results on the surface ionization of metastable calcium atoms on a polycrystalline tungsten surface. We demonstrate that metastable atoms undergo surface ionization with a greater efficiency than ground-state atoms. Metastable atoms can be selectively surface ionized with an appropriately selected electronic work function if $I_{\text{ex}} < \Phi < I_{\text{gs}}$, where I_{ex} is the ionization energy of the metastable state and I_{gs} is the ionization energy of the ground state. In alkaline earth and alkaline earth-like systems, this phenomenon has a direct application in atomic clocks, wherein a single frequency-stabilized laser is used to pump a narrow clock transition and the selective surface ionization of the resultant metastable atoms may yield a markedly higher signal-to-noise ratio than conventional atomic clock configurations.¹³

Furthermore, the ability to selectively ionize excited atoms on a metal surface can be exploited for isotope-selective detection and isotope enrichment: atoms of the desired isotope may be optically pumped by a resonant laser to an excited state. With an appropriately selected metal surface, the surface ionization efficiency may be significantly higher for the excited atoms.^{14,15}

Such an approach to enable the surface ionization of metastable atoms has the potential to be developed into a means of enriching specific calcium isotopes. The benefits of this approach are readily apparent in medicine, where calcium isotopes are routinely used to diagnose calcium absorption and metabolism disorders.^{16,17} Furthermore, when selectively exciting individual isotopes to metastable states, our approach may be used in conjunction with an ion optics system to extract, collect, and thereby enrich atoms of the desired isotope. Calcium compounds enriched with Ca-48 have a number of applications in fundamental science pertaining to the detection of neutrinoless double-beta decay.^{18,19}

II. EXPERIMENTAL SETUP

A schematic diagram of the setup is shown in Fig. 1. Calcium granules are vaporized in a capillary oven and a fraction of the atoms in the resulting beam are excited to the metastable $4s4p\ ^3P_J$ triplet in a glow discharge.^{20,21} A pair of transverse parallel plates about 15 cm downstream from the discharge is used to extract all charged particles remaining in the beam. The atomic beam subsequently impinges on a surface ionization apparatus (SIA) consisting of a polycrystalline tungsten wire as the ionizing surface and a surrounding stainless steel ion detector. The oven and tungsten wire within the SIA are operated at temperatures not exceeding 650°C and 1750°C, respectively. The pressure in the vacuum chamber, as monitored by two gauges, was on the order of 10^{-7} Torr after stabilizing for several hours. At this pressure, there was a persistent oxygen signal as measured by a residual gas analyzer.

The oven nozzle consists of a hexagonal array of twenty-eight capillaries (1.14 mm diameter, 48.3 mm length) packed into a triangular aperture.²² In order to meet the density requirements 1 cm downstream from the oven to ignite a self-sustained discharge, the oven was operated at a temperature of 650°C, yielding a beam with a calculated total flux

^{a)}Electronic mail: igalbucay@utexas.edu

of 2×10^{17} atoms/s and mean speed of 823.5 m/s, assuming a Maxwell-Boltzmann velocity distribution.^{20,23–25} Under these conditions, the effects of interatomic collisions on the beam dynamics may not be neglected and it is anticipated that the centerline intensity will be attenuated in proportion to the square root of the Knudsen number in conjunction with a broadening of the angular distribution of the beam.²⁵ The resultant angular spread of the beam was quantified using a quartz crystal thickness monitor from INFICON with a 1 mm aperture at the position of the surface ionization apparatus, approximately 26 cm downstream from the oven opening. The deposition data collected as the thickness monitor was scanned across the beam is shown in Fig. 2. The best fit to the data resembles the anticipated angular distribution of an effusive beam emanating from a single channel with an aspect ratio approximately 3.5 times less than the capillaries used in our source. This broader distribution is the result of using multiple capillaries at the oven opening and operating the oven in what is referred to as the transitional, or opaque, flow regime.²⁵ The enhanced number of atomic collisions resulting from both of these factors manifested as a broadening of the angular distribution of the beam. From this distribution, about 0.29% of the atoms in the beam impinge on the surface of the hot wire in the surface ionization apparatus per second.

III. RESULTS AND DISCUSSION

In lieu of a laser to pump the $4s^2 \ ^1S_0 \rightarrow 4s4p \ ^3P_1$ intercombination transition in calcium, we implemented a hollow-cathode discharge to populate the metastable 3P_J triplet. The discharge scheme consisted of a toroidal tungsten cathode and two high voltage anodes. The anodes are positioned approximately at approximately 2 cm increments from the grounded

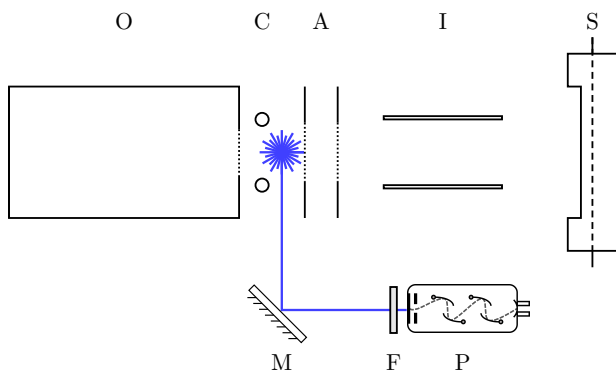


FIG. 1. Diagram of the experimental setup (not to scale). O: capillary oven heated by a heater cable wrapped around its body to about 650 °C. C: discharge cathode consisting of a 0.25 mm-diameter toroidal tungsten wire operated at 8.46 W. A: discharge anodes with a wire mesh spot-welded across their openings. I: ion extraction plates. S: surface ionization apparatus consisting of a stainless steel tube (ion detector) with a lateral rectangular cut and a coaxial hot tungsten wire (ionizing surface). M: mirror (other imaging optics not shown). F: bandpass filter centered around 442 nm. P: photomultiplier tube.

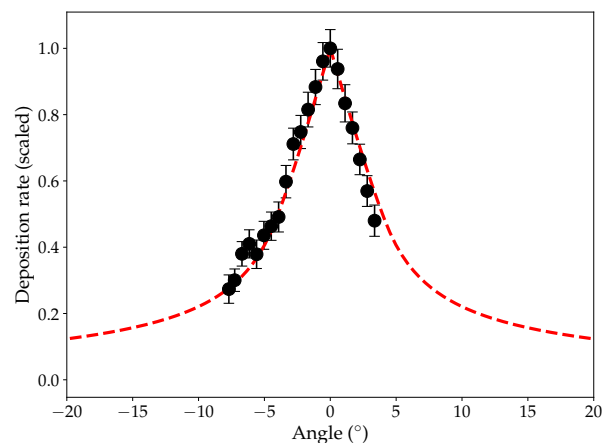


FIG. 2. Angular distribution of the atomic beam at the position of the SIA. Deposition rate data was collected at various positions with a thickness monitor while the discharge was on. The error bars denote the standard error in the deposition rate over a time span of five minutes. The red-dashed distribution is a best-fit to the data and corresponds to the distribution of an effusive source emanating from a channel with an aspect ratio 3.5 times less than the capillaries used in this experiment.²⁵

oven opening. 80% transmission wire meshes were spot welded across the opening of the anodes. Igniting a glow discharge depends largely on the electrode spacing and, more importantly, on the density of the gas between the electrodes. The experimental conditions must guarantee that the electron mean free path through the gas between the electrodes is long enough to enable the electrons to acquire the necessary kinetic energy for ionizing an atom and short enough to support multiple collisions before the electrons impinge on the anode. Since the gas density can be more easily modulated in-situ via the temperature, Giusfredi et. al. provide a lower limit for producing a self-sustained glow discharge:²⁰

$$n \geq \frac{1}{l\sigma_i} \sqrt{\frac{m_e}{m_i}}, \quad (2)$$

where n is the atomic density, l is the distance between the electrodes, σ_i is the electron-impact ionization cross section, m_e is the electron mass, and m_i is the ionic mass. These experimental conditions support an avalanche chain reaction of ionization events – a necessary prerequisite of a glow discharge. The transition to a self-sustaining glow discharge is accomplished when (a) the energy loss due to inelastic collisions with the gas atoms is recouped from higher external electric fields and (b) electron losses at the anode are compensated by enhanced electron emission at the cathode. The cathode may emit additional electrons due to secondary electron emission resulting from the impact of high energy ions or thermionic emission (i.e., a hot cathode).^{26–28} At our discharge length of $l \approx 2$ cm, and an ionization cross section of $\sigma_i \approx 5 \text{ \AA}^2$, the minimum atomic density for calcium is $\sim 3.7 \times 10^{18}$ atoms/m³. Naturally, due to the free expansion of the vapor into the vacuum chamber, the beam density outside of the oven will be

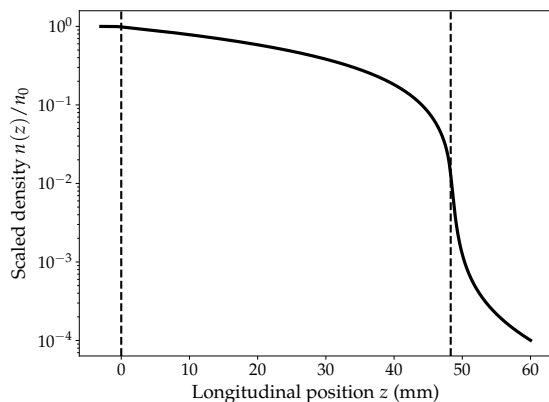


FIG. 3. Longitudinal density profile of a beam emanating from a single capillary with diameter $2r = 1.14$ mm and length $L = 48.3$ mm. The density along the axis of the capillary, $n(z)$, has been scaled by the density of the vapor within the reservoir, n_0 . The entrance and exit of the capillary have been marked by dashed lines at $z = 0$ and $z = L$, respectively.

significantly lower than $n = p(T_{\text{oven}})/kT_{\text{oven}}$. The density profile of an atomic beam drops by up to two orders of magnitude in the discharge region. For example, Fig. 3 demonstrates the calculated longitudinal density profile of a single capillary.²⁹ Consequently, the oven temperature must be sufficiently high to guarantee that the beam density meets the condition above for a glow discharge. We found this temperature empirically to be about 650 °C.

The electron-atom collisions within the discharge can impact several beam properties, particularly the beam angular spread and velocity distributions. Collisions between atoms and electrons traveling in the forward direction parallel to the atomic beam will simply result in a small longitudinal momentum transfer to the atom. In the event that an electron is scattered through some finite angle, the atom will receive a transverse momentum kick, which will manifest as a net increase in the angular spread of the beam, albeit by a small amount. Rundel, et. al. reported that electron-atom collisions in their discharge resulted in a 1.4° increase in the full-width half-maximum in the angular distribution of their metastable noble gas beam.³⁰ Furthermore, we expect a shift toward higher velocities in the velocity distribution of the beam as slower atoms will sustain greater angular deflections than faster atoms and consequently be more strongly attenuated.^{30,31}

In order to investigate the surface ionization of metastable atoms, it was necessary to quantify the fraction of atoms in the beam excited to metastable states. Considering the diffuse fluorescence signal of the decay of the 3P_1 state and the excessive background noise at this wavelength from the blackbody radiation of the oven, it proved impractical to use the fluorescence of the intercombination transition to estimate the total number of metastable atoms in the beam. We instead used a photomultiplier tube (Hamamatsu R212) and a bandpass filter (Edmund Optics part no.: 65-684) centered around 442 nm to measure

the intensity of the $^3D_J \rightarrow ^3P_J$ transitions as the background noise at these wavelengths was greatly reduced. The solid angle of our optical system was limited by a lens succeeding the mirror in Fig. 1 (not shown) to 0.04 sr, limiting the optical throughput of the system to approximately 0.23%. The dependence of this signal on the potential of the discharge anode with a constant current on the cathode is shown in Fig. 5. The presence of the cathode as a source of thermionic electrons was found to not have a significant impact on the $^3D_J \rightarrow ^3P_J$ transition intensity, as the glow discharge was readily ignited with the high voltage anodes alone. Of the 2×10^{17} atoms/s produced by the oven under aforementioned conditions, it is estimated that approximately 0.24% of the atoms undergo these transitions to the metastable 3P_J triplet. This is strictly a lower limit to the number of metastable atoms in the beam following the discharge for two reasons: not all atoms decay to the metastable triplet via 3D_J states and our detection system is insensitive to the metastable 1D_2 singlet state, which is also expected to undergo surface ionization along with the atoms in the 3P_J states. Furthermore, any ions produced by the discharge are extracted from the beam by a pair of parallel plates to prevent them from masking the surface ion signal at the SIA.

The design of the SIA has been described in more detail in an earlier article³⁶ and is depicted in Fig. 6. The SIA consists

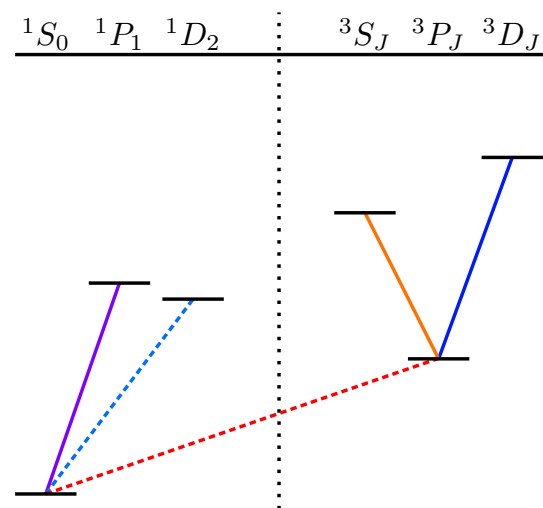


FIG. 4. Energy level diagram for calcium. The states we aim to populate with the discharge are the 3P_J states.

Initial	Final	Wavelength (nm)	A (s^{-1})	Reference
1P_1	1S_0	422.8	2.18×10^8	32
1P_1	1D_2	5547	2180	32
1D_2	1S_0	457	40	32
1D_2	$^3P_{1,2}$		96-300	32
3P_1	1S_0	657.4	2300	33, 34
$^3D_{1,2,3}$	$^3P_{0,1,2}$	442.7-445.8	10^7	35

TABLE I. Wavelengths and rates of spontaneous decay for relevant transitions in calcium.

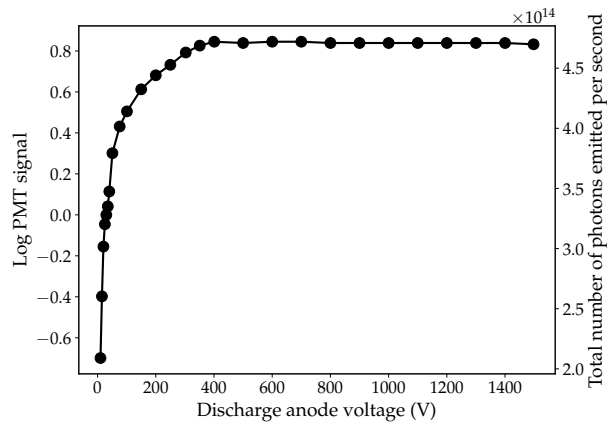


FIG. 5. Fluorescence signal from the 442 – 446 nm decays of the $^3D_J \rightarrow ^3P_J$ transitions. At saturation, approximately 0.24% of the atoms undergo these transitions.

of a hot, ionizing tungsten wire surrounded by a cylindrical stainless steel ion detector (collector) with a lateral rectangular cut to allow the atomic beam to be deposited onto the wire. Prior to any measurements, the hot wire was preconditioned for several hours at an approximate temperature of 2000 K. We measured the work function of the tungsten hot wire by measuring the thermionic emission of electrons at various temperatures. Throughout these measurements, the SIA was not exposed to the calcium beam. A Richardson plot of the data is displayed in Fig. 7, where the slope of the best fit to the data in the Richardson regime (in contrast to the space-charge or field-limited regime) yields the work function $\Phi = 5.18 \pm 0.03$ eV. This elevated value compared to the accepted work function of clean polycrystalline tungsten (4.54 eV) is likely a result of partial surface oxidation. Indeed, at a background pressure of 10^{-7} Torr, we may expect an increase in the tungsten work function of up to ~ 0.9 eV.³⁷

Nonetheless, this work function change should not constitute a significant problem. According to Eq. 1 and elemental surface ionization theory, even with partial oxidation, it is still expected that the metastable calcium atoms be surface ionized with a much greater efficiency than the ground state atoms. Here, it should also be noted that the work function measurements via the positive thermal ionization of gaseous atomic species with known ionization energies are in general agreement with those of thermionic emission of electrons.^{1,8,10,38–40}

In addition to its effect on the work function, oxidation will have an additional impact on surface ionization efficiency through its effect on desorption dynamics and chemical reactivity at the surface. For ground-state calcium atoms on a rhenium hot wire, Stienkemeier, et. al., report a diminished surface ionization efficiency at wire temperatures exceeding ~ 1900 K, which they attribute to enhanced oxide formation.⁵ Since we can only assume that metastable calcium atoms and their ensuing ions will also exhibit increased reactivity with oxygen at these temperatures, we operated our tungsten hot wire at a temperature of 1750 K.

Furthermore, surface contamination is known to affect des-

orption lifetimes.⁴¹ The mean residence time $\tau_{i,a}$ of an atom or ion adsorbed on a surface with adsorption energy $E_{i,a}$ at temperature T is given by the Arrhenius equation:

$$\tau_{i,a} = \tau_0 e^{E_{i,a}/k_B T}, \quad (3)$$

where τ_0 is a desorption time constant on the order of $\sim 10^{-16} - 10^{-13}$ s depending on the surface mobility of the adsorbates.^{5,6,42} Calcium and other alkaline earth atoms exhibit relatively more localized behavior with a prefactor τ_0 on the order of 10^{-13} s. For alkali atoms, it has been demonstrated that the desorption time decreases with an increase in the oxidation of the surface since the oxygen serves as an intermediate layer, effectively increasing the distance between the alkali atoms and the hot wire surface.⁴¹ Presumably, this effect is present between the calcium atoms and our partly oxygenated tungsten wire. Ultimately, the desorption time of the metastable calcium atoms must be sufficiently long to allow for surface ionization, while not exceeding some limit beyond which the ion may be neutralized through an additional charge exchange interaction before evaporating from the hot wire. Further work needs to be done in order to establish the optimal desorption conditions for the surface ionization of metastable atoms.

The work function measurements of Fig. 7 were performed under a background pressure of 10^{-7} Torr and while the calcium beam was obstructed. The reasoning for the latter is that the electric field between the electrodes in the SIA (that is, the tungsten hot wire and the surrounding detector) was reversed during the work function measurements to enable to emission

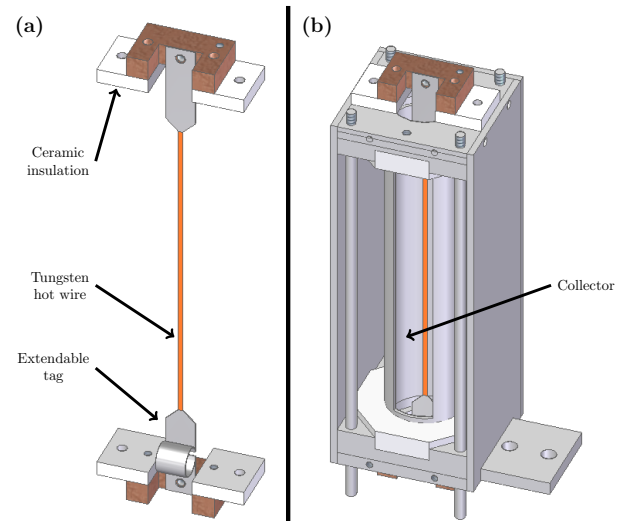


FIG. 6. (a) Bare tungsten hot wire and (b) the fully assembled SIA. The tungsten hot wire is spot welded onto two molybdenum pieces, one of which is extendable to accommodate any change in strain resulting from the thermal expansion of the hot wire. The hot wire is surrounded by a cylindrical stainless steel ion detector (collector) with a lateral rectangular opening to allow the atomic beam to impinge on the hot wire. Custom-machined ceramic parts were used to isolate the hot wire and collector from the grounded frame on the exterior of the SIA.

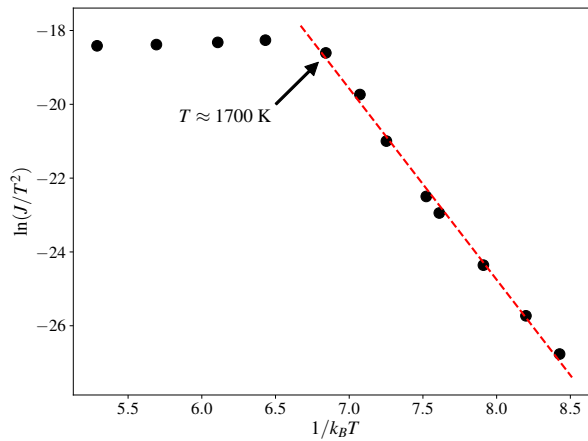


FIG. 7. A Richardson plot of thermionic emission of electrons from a polycrystalline tungsten hot wire. For the work function measurement, the hot wire was floated to 100 V and the surrounding stainless steel detector was grounded through an ammeter. The slope of the thermionic electron current with respect to temperature in the Richardson regime yields the work function of the wire. The data for temperatures above 1700 K are evidently space-charge limited.

of thermionic electrons. Specifically, the hot wire was floated to 100 V and the surrounding detector was grounded. The calcium beam was obstructed because this electric field would hinder the evaporation of any ions formed at the surface, leading to an anomalous accumulation of calcium ions on the hot wire that is not otherwise present in this experiment. Naturally, the accumulation of neutral calcium may still occur during the work function measurements as well as the rest of the experiment since it is independent of the electric field within the SIA. However, since the hot wire temperature is much greater than that of the calcium oven, neutral calcium accumulation on the tungsten surface is insignificant since the rate of evaporation exceeds the rate of adsorption. In any case, we want to emphasize that the results in Fig. 7 were consistent with time and reproducible under the experimental conditions mentioned above.

Fig. 8 presents the dependence of the surface ionization signal at the SIA on the potential of the discharge anode. When collecting this data, the discharge cathode was heated to the same temperature as in Fig. 5 and the field between ion extraction parallel plates was maintained at 200 V/mm. In contrast to the aforementioned work function measurements, the surface ion current was anticipated to be several orders of magnitude less than the thermionic electron current. We correspondingly used a Femto low noise transimpedance amplifier with a variable gain, which allowed the stainless steel detector to be floated at -10 V. The detected surface ion current increased with the voltage on the discharge anode until saturating at about 400 V, the same saturation voltage in Fig. 5.

To demonstrate that the SIA ion signal in Fig. 9 is due exclusively to the surface ionization of metastable atoms and is not obscured by ions originating from the plasma in the discharge, we operated the discharge with 1 kV on the discharge anode and modulated the field between the ion extrac-

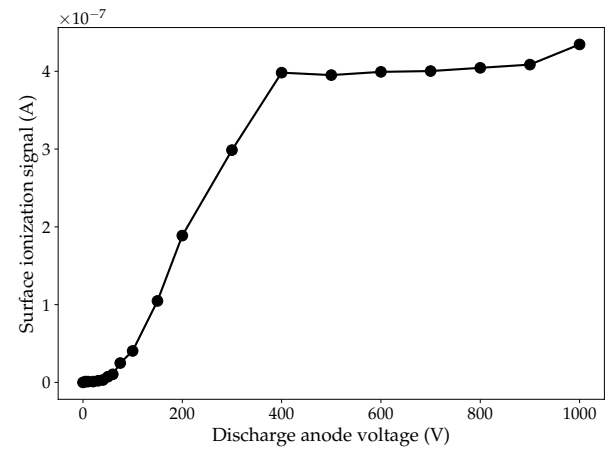


FIG. 8. Surface ion signal at the SIA as a function of the discharge anode voltage. The field between the ion extraction plates was 200 V/mm. As the discharge anode voltage increased, the fraction of metastable atoms in the beam inferred from the fluorescence data in Fig. 5 also increased, until reaching saturation at 400 V.

tion plates. From the discharge fluorescence measurements in Fig. 5, we estimated that about 0.24% of the atoms in the beam were excited to the 3P_J states at these conditions and that some fraction of the atoms were ionized by electron bombardment. With no field between the ion extraction plates, the SIA ion signal was overwhelmed by the discharge ions. As the ion extraction field increased, the SIA ion signal quickly decreased to approximately 500 nA. Naturally, modulating the ion extraction field while the discharge was off did not have a noticeable effect on the SIA signal. Ion extraction fields of 25 V/mm and above are sufficiently strong to deflect all discharge ions and preclude them from impinging on the SIA ion collector. The 500 nA current is readily attributable to the surface ionization of metastable calcium atoms.

At the aforementioned operating conditions (oven temperature 650 °C, discharge anode voltage 1 kV, constant discharge cathode temperature), fluorescence measurements indicated that approximately 0.24% of the atoms in the atomic beam are excited to a metastable state. From the data in Fig. 2, approximately 0.29% of the total flux of emitted atoms impinge on the 0.25 mm-diameter hot wire positioned at a distance of 26 cm from the oven opening. It follows that 1.4×10^{12} metastable atoms land on the tungsten hot wire per second. Recall this is a lower limit to the number of metastable atoms in the beam as not all atoms decay to the metastable triplet via the $^3D_J \rightarrow ^3P_J$ transitions and our detection system is insensitive to the metastable 1D_2 singlet state, which is also expected to undergo surface ionization along with the atoms in the 3P_J states. The work function of the polycrystalline tungsten hot wire was determined through thermionic emission to be $\Phi = 5.18 \pm 0.03$ eV – an appropriate value that exceeds the ionization energy of the metastable state, while maintaining a sufficiently low probability of ionization for the ground state atoms. Indeed, according to Eq. 1, we may expect up to 0.5% of ground state calcium atoms impinging on the tungsten hot wire to undergo ionization. This current manifests as a con-

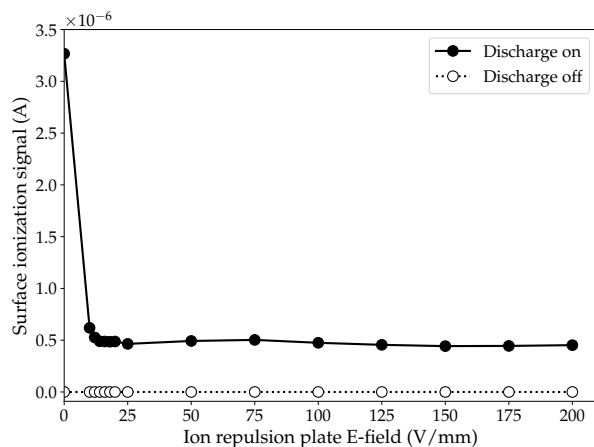


FIG. 9. Surface ion signal as a function of the field between the ion extraction plates. For the black data set, the discharge anode was held at a potential of 1000 V. At an ion extraction field of zero, ions produced by electron bombardment in the discharge are detected by the SIA and mask the metastable atom surface ion signal. Increasing the potential difference between the ion extraction plates progressively deflected the discharge ions away from the SIA, revealing a finite signal corresponding to the surface ionization of metastable calcium. The white data set was collected under the same conditions, albeit with a discharge anode voltage of 0 V.

stant background signal in Fig. 8 and 9 that we measured to be on the order of ~ 1 nA. We may further suppress this background signal by using a hot wire with a lower work function – this may be accomplished by attaining a lower background pressure to reduce the effects of oxidation or by using a metal with a lower work function (e.g., molybdenum).³⁷

The 500 nA surface ion current in Fig. 9 corresponds to an ion flux of about 3.1×10^{12} ions/s. This high current can be readily explained by noting that the fluorescence measurements of metastable atoms are strictly underestimates for two reasons. First, the fluorescence detection setup was only sensitive to the $^3D_J \rightarrow ^3P_J$ transitions. There is no compelling reason to assume that these transitions account for all atoms excited to the metastable 3P_J triplet in the discharge: some may be directly excited to the 3P_J triplet and others may decay via the 3S_1 triplet (see Fig. 4). Second, some unknown fraction of atoms are excited to the metastable 1D_2 singlet – atoms which cannot be detected yet undergo ionization along with the 3P_J atoms (see Tab. I). This is due to the fact that surface ionization is a non-resonant process and any atom with an ionization energy less than the work function of a surface will have a high probability of undergoing surface ionization. When considering two distinct atomic states of calcium, such as the 1D_2 and 3P_J metastable states, both have a high probability of ionization according to Eq. 1. It is therefore not possible to selectively ionize atoms in either metastable state and all metastable states contribute to the ion current at the SIA.

Despite these limitations in the fluorescence measurements, the experiment outlined in this report indicates that metastable calcium atoms experience a high degree of ionization on a

tungsten surface and we may conclude that the efficiency of the surface ionization of metastable calcium atoms is appreciably higher than that of the corresponding ground state atoms. Effectively, metastable atoms can be selectively ionized by a hot metal surface with an appropriate work function. This has potential applications for improved signal-to-noise ratios in frequency standards by using a single laser to pump clock transitions in alkaline earth and alkaline earth-like systems, followed by selective surface ionization to detect the excited atoms.

Here, it is necessary to acknowledge potential limitations to the applicability of this selective surface ionization mechanism to other atomic species. This report demonstrates that to a large extent, it is the relationship between the effective ionization energy of the metastable state and the surface work function that determines the probability of surface ionization. However, in the event that the excitation energy of the metastable atom is comparable to or exceeds the work function of the surface, additional charge exchange processes may occur, specifically Auger neutralization. Auger neutralization will occur with a high probability if the ion recombination energy to the ground state exceeds double the work function, $E^+ \geq 2\Phi$, at which point an electron from the metal surface tunnels to the vacant ground state of the surface ion. The excess energy from Auger neutralization simultaneously excites a separate electron to a higher energy band in the metal. If the excess energy is sufficiently high, this Auger electron may be ejected from the metal and used in spectroscopy or for metastable atom detection.^{43–47} A process such as Auger neutralization preclude the use of surface ionization in the applications mentioned above for certain atomic species (e.g., metastable noble gas atoms, which are readily neutralized following ionization). While surface ionization may too be used for metastable atom detection (through ion emission, in contrast to electron emission),⁴⁸ ion emission is necessary for application to atomic clocks and isotope enrichment, which necessarily require the surface ion to desorb from the surface without undergoing a neutralizing charge exchange. In the case of the isotope enrichment of calcium, for example, atoms of a particular isotope such as Ca-48 may be optically pumped to the metastable 3P_1 state. These metastable atoms may then be selectively ionized at a hot surface with a high work function and subsequently guided to a collector. Such a scheme would not be feasible for certain atomic species with a high probability of undergoing Auger neutralization after ionization, such as metastable noble gas atoms.^{44,47}

IV. CONCLUSION

In conclusion, we have demonstrated that metastable calcium atoms undergo surface ionization on a hot tungsten surface with a markedly greater efficiency than ground state calcium atoms. Here, we excite a fraction of calcium atoms in a thermal beam to metastable 3P_J states through a glow discharge and we estimate the number of metastable atoms by detecting the fluorescence of the decays of higher-lying 3D_J states. These measurements provide an underestimate for the

fraction of metastable atoms in the beam. The ground and excited atoms then impinge on a polycrystalline tungsten hot wire with a work function measured to be $\Phi = 5.18 \pm 0.03$ eV. Ions evaporating from the hot wire surface are then detected as a current by a stainless steel sheath enveloping the hot wire. In light of the fact that the fluorescence measurements inherently underestimate the flux of metastable atoms in the beam, it is evident that the surface ionization of metastable calcium atoms is high. These results can be used to develop novel isotope enrichment methods and compact atomic clocks. In particular, stable isotopes of calcium have garnered appreciable attention for their use in medicine and basic scientific research.^{16–19} These applications have, in turn, spurred several experiments focused on calcium isotopes.^{49–51}

Data availability statement

The data that support the findings of this study are available from the corresponding author upon reasonable request.

- ¹M. Kaminsky, *Atomic and ionic impact phenomena on metal surfaces* (Academic Press, Inc., 1965).
- ²R. Delhuille, A. Miffre, E. Lavallette, M. Büchner, C. Rizzo, G. Tréneç, J. Vigué, H. J. Loesch, and J. P. Gauyacq, "Optimization of a Langmuir-Taylor detector for lithium," *Rev. Sci. Instrum.* **73**, 2249–2258 (2002).
- ³M. J. Dresser, "The Saha-Langmuir equation and its application," *J. Appl. Phys.* **39**, 338–339 (1968).
- ⁴I. Langmuir and K. Kingdon, "Thermionic effects caused by vapours of alkali metals," *Proc. R. Soc. London. Ser. A.* **107**, 61–79 (1925).
- ⁵F. Stienkemeier, M. Wewer, F. Meier, and H. O. Lutz, "Langmuir–Taylor surface ionization of alkali (Li, Na, K) and alkaline earth (Ca, Sr, Ba) atoms attached to helium droplets," *Rev. Sci. Instrum.* **71**, 3480–3484 (2000).
- ⁶M. Scheer, R. Klein, and J. McKinley, "Surface lifetimes of alkali metals on molybdenum," *J. Chem. Phys.* **55**, 3577–3584 (1971).
- ⁷L. Schmidt and R. Gomer, "Neutral and ionic desorption of cesium from tungsten," *J. Chem. Phys.* **43**, 2055–2063 (1965).
- ⁸M. Dresser and D. Hudson, "Surface ionization of some rare earths on tungsten," *Phys. Rev.* **137**, 673–682 (1965).
- ⁹G. D. Alton, "Characterization of a cesium surface ionization source with a porous tungsten ionizer. I," *Rev. Sci. Instrum.* **59**, 1039–1044 (1988).
- ¹⁰H. Kawano, S. Matsui, and N. Serizawa, "Thermal positive-ion source developed for molecular beam detection," *Rev. Sci. Instrum.* **67**, 1193–1195 (1996).
- ¹¹M. Laatiaoui, H. Backe, M. Block, F.-P. Heßberger, P. Kunz, F. Lautenschläger, W. Lauth, M. Sewtz, and T. Walther, "On laser spectroscopy of the element nobelium ($z = 102$)," *Eur. Phys. J. D* **68**, 71 (2014).
- ¹²T. K. Sato, M. Asai, A. Borschevsky, T. Stora, N. Sato, Y. Kaneya, K. Tsukada, C. Düllman, K. Eberhardt, E. Eliav, S. Ichikawa, U. Kaldor, J. V. Kratz, S. Miyashita, Y. Nagame, K. Ooe, A. Osa, D. Renisch, J. Runke, M. Schädel, P. Thörle-Pospiech, A. Toyoshima, and N. Trautmann, "Measurement of the first ionization potential of lawrencium, element 103," *Nature* **520**, 209–211 (2015).
- ¹³H. Shang, X. Zhang, S. Zhang, D. Pan, H. Chen, and J. Chen, "Miniaturized calcium beam optical frequency standard using fully-sealed vacuum tube with 10^{-15} instability," *Opt. Express* **25**, 30459–30467 (2017).
- ¹⁴F. Schwirzke, U.S. Patent No. 4,394,579 (19 Jul. 1983).
- ¹⁵B. Auschwitz and K. Lacmann, "The ionization of excited sodium atoms on a tungsten surface," *Chem. Phys. Lett.* **113**, 9–12 (1985).
- ¹⁶J. Morgan, J. Skulan, G. Gordon, S. Romaniello, S. Smith, and A. Anbar, "Rapidly assessing changes in bone mineral balance using natural stable calcium isotopes," *Proc. Natl. Acad. Sci.* **109**, 9989–9994 (2012).
- ¹⁷P. Moser-Veillon, A. Mangels, N. Vieira, A. Yergey, K. Patterson, A. Hill, and C. Veillon, "Calcium fractional absorption and metabolism assessed using stable isotopes differ between postpartum and never pregnant women," *J. Nutr.* **131**, 2295–2299 (2001).
- ¹⁸F. Avignone, S. Elliott, and J. Engel, "Double beta decay, majorana neutrinos, and neutrino mass," *Rev. Mod. Phys.* **80**, 481–516 (2008).
- ¹⁹Y. Iwata, N. Shimizu, T. Otsuka, Y. Utsuno, J. Menendez, M. Honma, and T. Abe, "Large-scale shell-model analysis of the neutrinoless $\beta\beta$ decay of ca-48," *Phys. Rev. Lett.* **116**, 1–6 (2016).
- ²⁰G. Giusfredi, A. Godone, E. Bava, C. Novero, and E. Sava, *J. Appl. Phys.* **63**, 1279–1285 (1988).
- ²¹J. V. B. Gomide, G. A. Garcia, F. C. Cruz, A. J. Polaquini, M. P. Arruda, D. Pereira, and A. Scalabrin, "Construction of an atomic beam system and efficient production of metastable states," *Brazilian J. Phys.* **27**, 266–275 (1997).
- ²²R. Senaratne, S. Rajagopal, Z. Geiger, K. Fujiwara, V. Lebedev, and D. Weld, "Effusive atomic oven nozzle design using an aligned microcapillary array," *Rev. Sci. Instrum.* **86**, 023105 (2014).
- ²³N. Ramsey, *Molecular beams*, 1st ed. (Oxford University Press, 1956).
- ²⁴J. Giordmaine and T. Wang, "Molecular beam formation by long parallel tubes," *J. Appl. Phys.* **31**, 463–471 (1960).
- ²⁵H. C. W. Beijerinck and N. F. Verster, "Velocity distribution and angular distribution of molecular beams from multichannel arrays," *J. Appl. Phys.* **46**, 2083–2091 (1975).
- ²⁶N. S. J. Braithwaite, "Introduction to gas discharges," *Plasma Sources Sci. Technol.* **9**, 517–527 (2000).
- ²⁷A. Bogaerts and R. Gijbels, "Modeling of metastable argon atoms in a direct-current glow discharge," *Phys. Rev. A* **52**, 3743–3751 (1995).
- ²⁸R. Franklin, *Plasma phenomena in gas discharges*, Oxford engineering science series (Clarendon, 1976).
- ²⁹H. Pauly, *Atom, molecule, and cluster beams I*, 1st ed. (Springer-Verlag Berlin Heidelberg, 2000).
- ³⁰R. D. Rundel, F. B. Dunning, and R. F. Stebbings, "Velocity distributions in metastable atom beams produced by coaxial electron impact," *Rev. Sci. Instrum.* **45**, 116–119 (1974).
- ³¹R. Freund and W. Klemperer, "Molecular beam time-of-flight measurements for the study of metastable atoms and repulsive electronic states," *J. Chem. Phys.* **47**, 2897–2904 (1967).
- ³²N. Beverini, F. Giammanco, E. Maccioni, F. Strumia, and G. Vissani, "Measurement of the calcium 1P₁-1D₂ transition rate in a laser-cooled atomic beam," *J. Opt. Soc. Am.* **6**, 2188–2193 (1989).
- ³³C. Degenhardt, H. Stoehr, C. Lisdat, G. Wilpers, H. Schnatz, B. Lipphardt, T. Nazarova, P. Pottie, U. Sterr, J. Helmcke, and F. Riehle, "Calcium optical frequency standard with ultracold atoms: Approaching 10^{-15} relative uncertainty," *Phys. Rev. A* **72**, 1–17 (2005).
- ³⁴L. Pasternack, D. M. Silver, D. R. Yarkony, and P. J. Dagdigan, "Experimental and theoretical study of the Ca I 4s3d 1D - 4s2 1S and 4s4p 3P₁ - 4s2 1S forbidden transitions," *J. Phys. B.* **13**, 2231–2241 (1980).
- ³⁵A. Kramida, Y. Ralchenko, J. Reader, and N. A. Team, "NIST Atomic Spectra Database (ver. 5.6.1)," (2018).
- ³⁶T. Mazur, B. Klappauf, and M. Raizen, "Demonstration of magnetically activated and guided isotope separation," *Nat. Phys.* **10**, 601–605 (2014).
- ³⁷H. Kawano, T. Takahashi, Y. Tagashira, H. Mine, and M. Moriyama, "Work function of refractory metals and its dependence upon working conditions," *Appl. Surf. Sci.* **146**, 105–108 (1999).
- ³⁸S. Datz and E. Taylor, "Ionization on platinum and tungsten surfaces. I. The alkali metals," *J. Chem. Phys.* **25**, 389–394 (1956).
- ³⁹J. Zemel, "Surface ionization phenomena on polycrystalline tungsten," *J. Chem. Phys.* **28**, 410–413 (1958).
- ⁴⁰H. Kawano, "Effective work functions for ionic and electronic emissions from mono- and polycrystalline surfaces," *Prog. Surf. Sci.* **83**, 1–165 (2008).
- ⁴¹H. L. Daley, A. Y. Yahikuru, and J. Perel, "K⁺, Na⁺, and Li⁺ desorption from oxygenated tungsten," *J. Chem. Phys.* **52**, 3357–3359 (1970).
- ⁴²M. Scheer and J. Fine, "Kinetics of desorption III. Rb⁺, K⁺, and Na⁺ on rhenium," *J. Chem. Phys.* **39**, 1752–1755 (1963).
- ⁴³W. Sesselmann, B. Woratschek, J. Küppers, G. Ertl, and H. Haberland, "Interaction of metastable noble-gas atoms with transition-metal surfaces: Resonance ionization and auger neutralization," *Phys. Rev. B* **35**, 1547–1559 (1987).
- ⁴⁴R. Monreal, D. Goebel, D. Primetzhofner, and P. Bauer, "Effects of the atomic level shift in the auger neutralization rates of noble metal surfaces," *Nucl. Instrum. Meth. B.* **315**, 206–212 (2013).

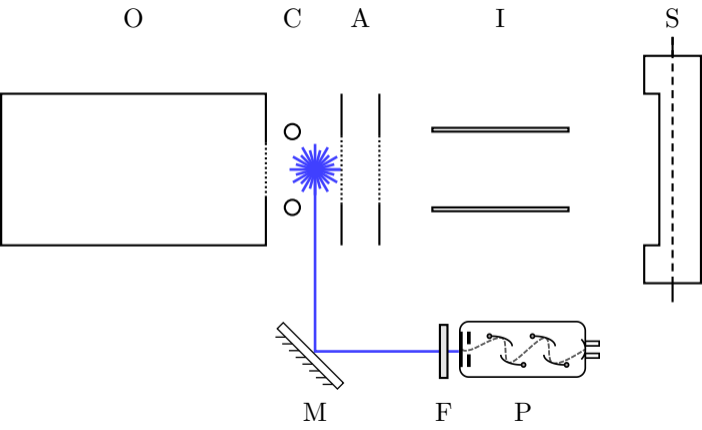
This is the author's peer reviewed, accepted manuscript. However, the online version of record will be different from this version once it has been copyedited and typeset.

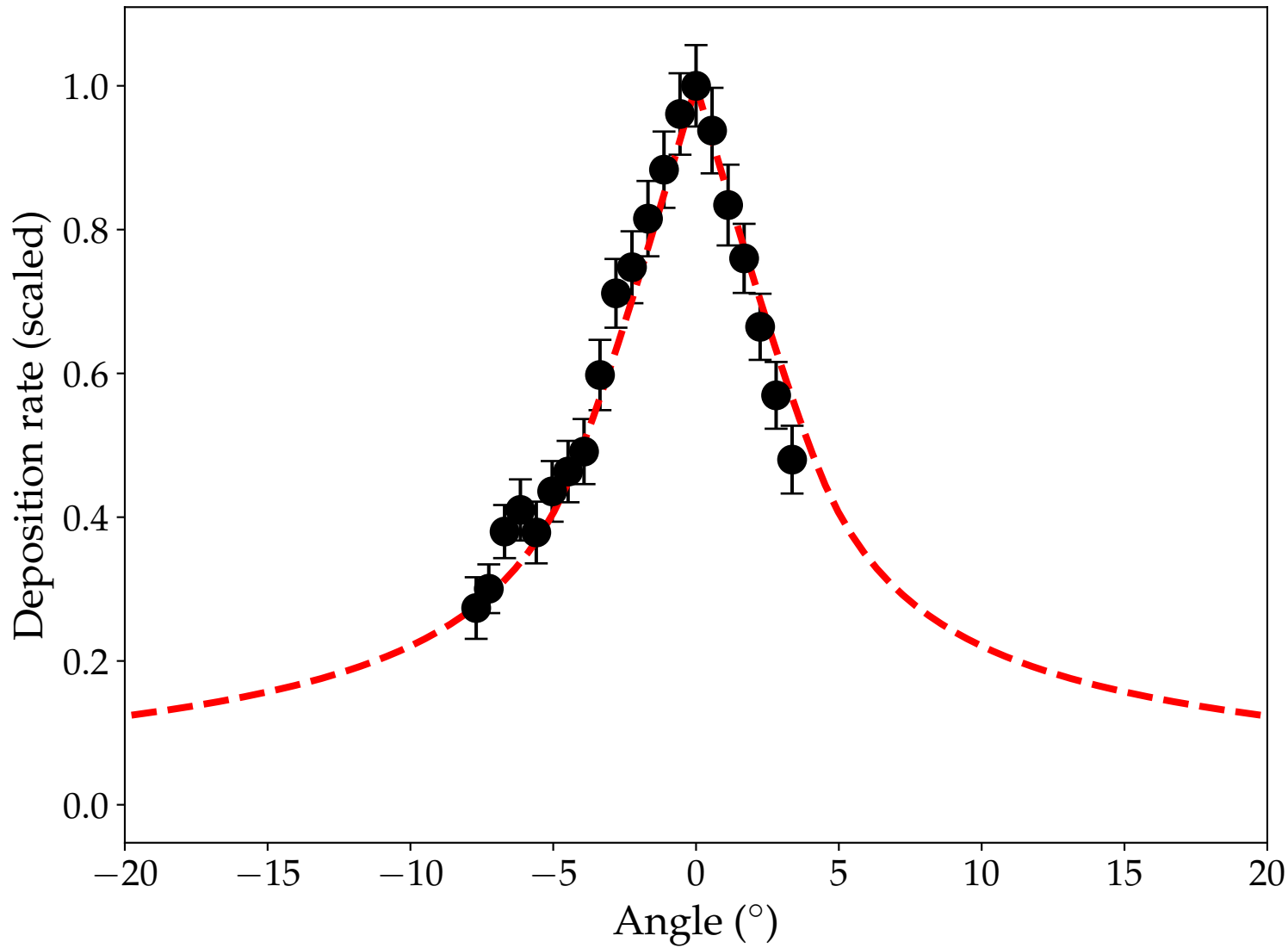
PLEASE CITE THIS ARTICLE AS DOI:10.1063/1.50005895

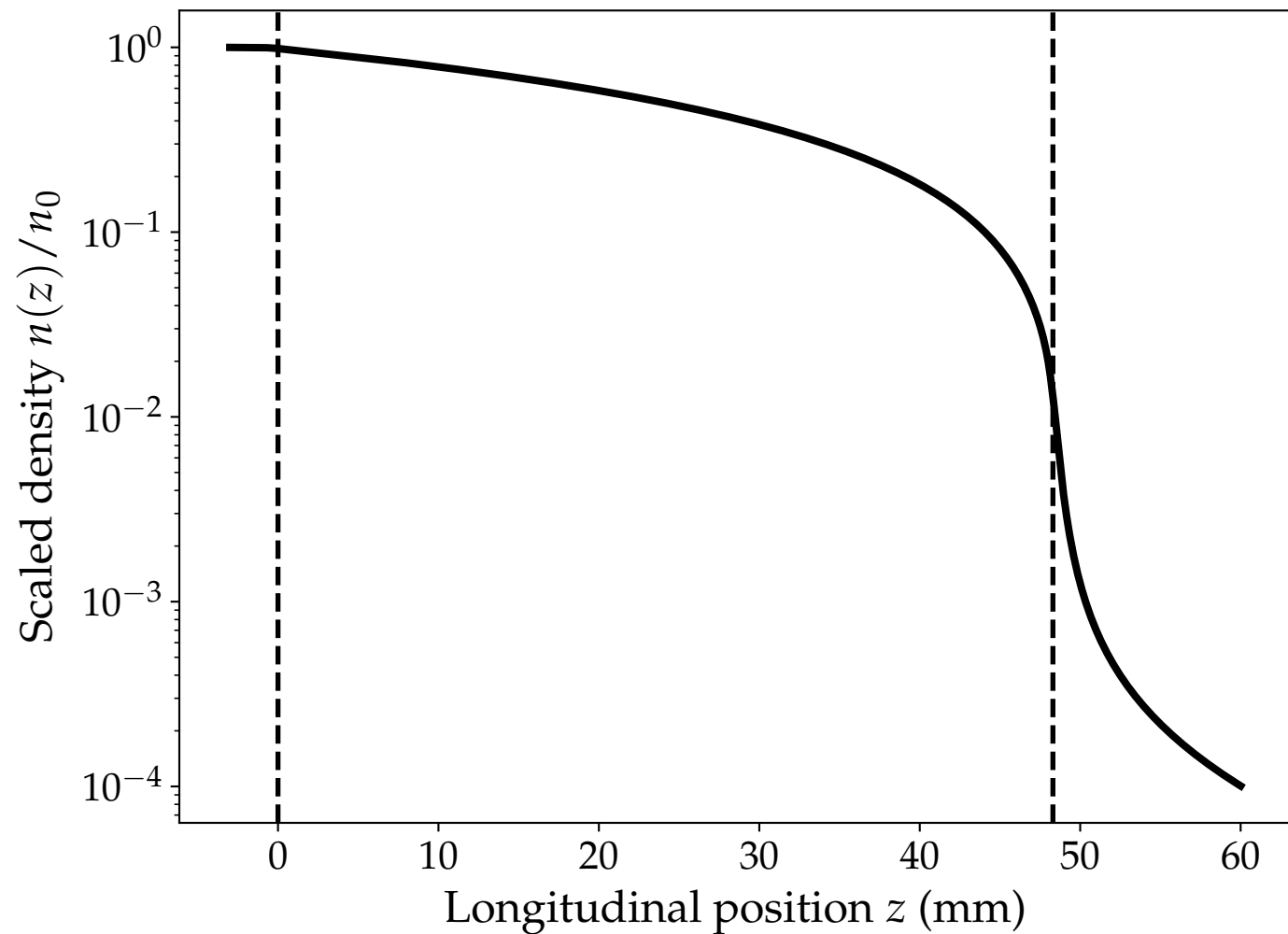
- ⁴⁵M. A. Cazalilla, N. Lorente, R. D. Muiño, J.-P. Gauyacq, D. Teillet-Billy, and P. M. Echenique, "Theory of auger neutralization and deexcitation of slow ions at metal surfaces," *Phys. Rev. B* **58**, 13991–14006 (1998).
- ⁴⁶H. D. Hagstrum, "Effect of monolayer adsorption on the ejection of electrons from metals by ions," *Phys. Rev.* **104**, 1516–1527 (1956).
- ⁴⁷H. D. Hagstrum, "Detection of metastable atoms and ions," *J. App. Phys.* **31**, 897–904 (1960).
- ⁴⁸K. Christandl, G. P. Lafyatis, A. Modoran, and T.-H. Shih, "Two-dimensional imaging of neutral alkali atom samples using surface ionization," *Rev. Sci. Instrum.* **73**, 4201–4205 (2002).
- ⁴⁹D. Lucas, A. Ramos, J. Home, M. McDonnell, S. Nakayama, J.-P. Stacey, S. Webster, D. Stacey, and A. Steane, "Isotope-selective photoionization

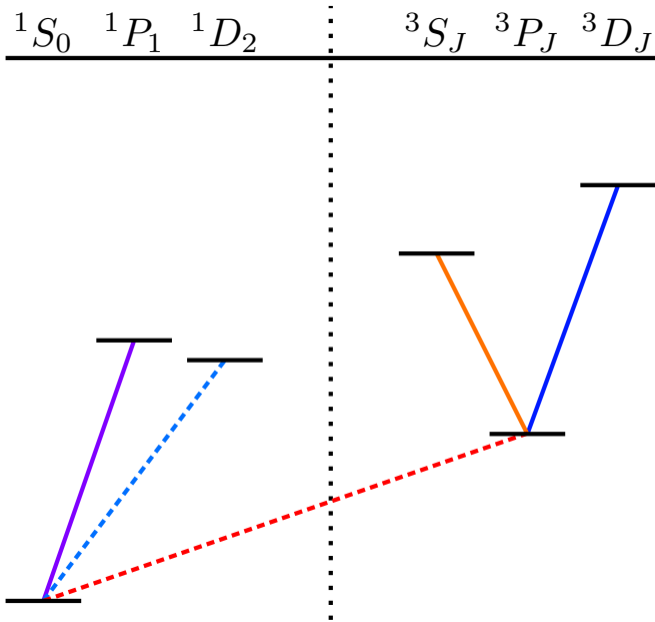
for calcium ion trapping," *Phys. Rev. A.* **69**, 012711 (2004).

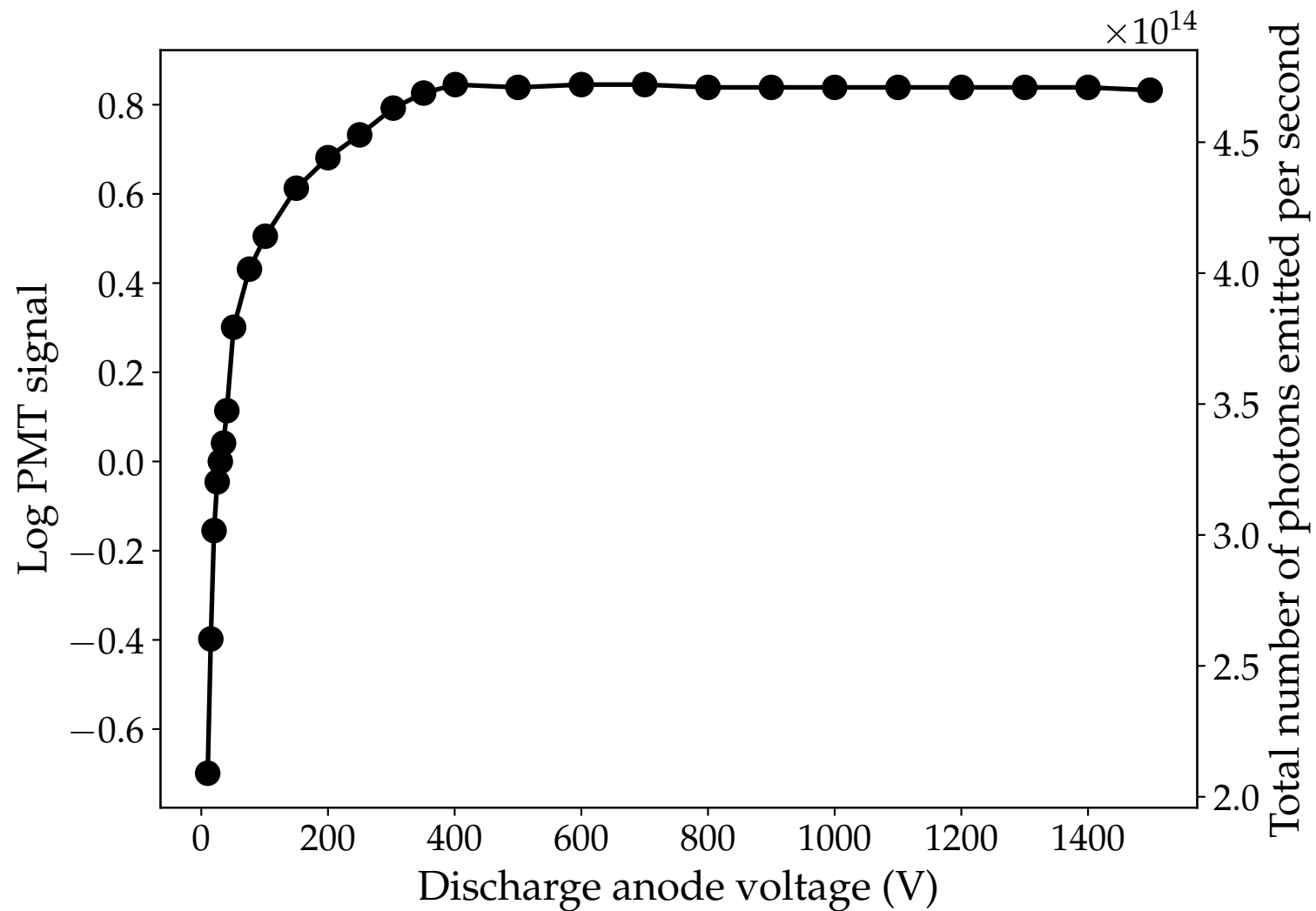
- ⁵⁰S. Hoekstra, A. Mollema, R. Morgenstern, H. Wilschut, and R. Hoekstra, "Single-atom detection of calcium isotopes by atom-trap trace analysis," *Phys. Rev. A.* **71**, 023409 (2005).
- ⁵¹R. Garcia-Ruiz, C. Gorges, M. Bissell, K. Blaum, W. Gins, H. Heylen, K. Koenig, S. Kaufmann, M. Kowalska, P. Krämer, Lievens, S. Malbrunot-Ettenauer, R. Neugart, G. Neyens, W. Nörtershäuser, D. Yordanov, and X. Yang, "Development of a sensitive setup for laser spectroscopy studies of very exotic calcium isotopes," *J. Phys. G: Nucl. Part. Phys.* **44**, 044003 (2017).



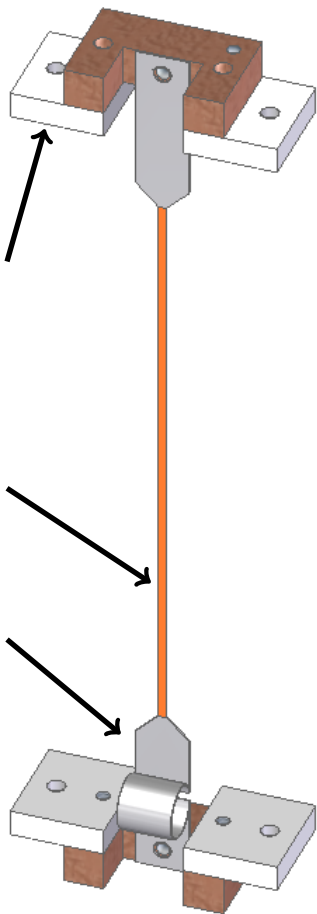








(a)



(b)

